Engineering Chemistry
ISSN: 2813-6535, Vol. 5, pp 1-11
doi:10.4028/p-AuNW19

Submitted: 2022-09-23
Revised: 2023-04-08
Accepted: 2023-06-14
Online: 2024-01-19

The Effect of Sodium Acetate on Biodegradable Rice Starch-Based Solid Polymer Electrolyte for Supercapacitor

Agung Nugroho[1,a], Muchammad Syaifudin[1,b], and Sylvia Ayu Pradanawati[2,c*]

[1]Chemical Engineering Department, Universitas Pertamina, Indonesia

[2]Mechanical Engineering Department, Universitas Pertamina, Indonesia

[a]agung.n@universitaspertamina.ac.id, [b]chammadsyaifudin@gmail.com, [c]sylvia.pradanawati@universitaspertamina.ac.id,

Keywords: Amorphous, ionic conductivity, rice starch, salt, sodium acetate, solid polymer electrolyte, supercapacitor

Abstract. This study examined the use of sodium acetate salt as an ionic dopant in biodegradable solid polymer electrolyte (SPE). In the solution casting method for making polymer electrolyte, rice starch is used as the host polymer and glycerol is used as the plasticizer. The characteristics of SPE film were investigated using X-Ray Diffraction (XRD), Fourier Transform Infrared (FT-IR), and Thermogravimetric Analysis (TGA). Salt enhances the amorphous structure by decreasing the crystallinity of the polymer. Alternatively, it decreases the temperature of thermal breakdown. In addition, the biodegradability of SPE was investigated using the soil burial method. Electrochemical Impedance Spectroscopy (EIS) was used to evaluate the ionic conductivity behavior and temperature dependent of SPE. The 35% sodium acetate salt addition makes the supercapacitor's electrolyte have the highest ionic conductivity at room temperature, which is 5.57×10^{-4} S/cm.

Introduction

Supercapacitor has promising potential as energy storage system for renewable energy plant. It has the ability to store about 10–100 times more energy per unit volume than ordinary capacitors and has a faster charge transfer rate than batteries [1]. In supercapacitor, there are several problems encountered such as leaks and limited size design when using liquid electrolyte. Therefore, researchers are investigating various solid polymer electrolytes (SPE) as suitable replacements for liquid electrolytes. SPE has environmentally friendly properties because it uses natural raw materials that are non-toxic, biodegradable, and sustainable based material. Organic polymers can be generally extracted directly from biomass such as starch, cellulose, and chitosan [2]. In this study, starch will be used as the host polymer for preparing solid electrolytes because it has lower glass transition temperature than chitosan and cellulose [3]. In SPE synthesis, lower glass transition temperature is more preferred because it can make the ionic conductivity increase. This is because the movement and flexibility of polymer chains are higher in polymer matrix that have a low glass transition temperature [3].

The source of starch used in this research is derived from rice because it has the highest amylose content compared to other starches [4]. The concentration of amylose in rice starch is 35%, and that of amylopectin is 65% [4]. The content of amylose and amylopectin plays a role in the crystalline and amorphous structure of starch. Amylose corresponds to the amorphous structure of starch since it has a linear chain while amylopectin corresponds in the crystal structure of starch because of its branched chain. Therefore, starch with higher amylose content has more amorphous structure [5]. In SPE synthesis, starch with higher amylose content has higher ion mobility since ions from the addition of salts attack more on the amylose unit [6].

In general, solid electrolytes derived from biomass polymers have low ionic conductivity. Therefore, it requires the addition of salt as an ionic dopant to improve the ionic conductivity. Commonly, the salt used as ionic dopant is lithium (Li) salt, but this salt is dangerous and limited availability in nature. In this study, ionic dopants based on sodium salt (Na) were used because they are abundant in nature, cheap, and environmentally friendly and also have chemical properties similar

to lithium [7]. In addition, based on comparative studies conducted by Osman et al. [8] showed that sodium-based electrolyte systems have a higher ionic conductivity compared to lithium-based electrolyte systems at room temperature. This is due to Na^+ has lower energy lattice compared to Li^+, therefore sodium-based salts are more conductive and more mobile in matrix polymer. Based on previous research written by Khanmirzaei et al. [6], it was obtained that the highest ionic conductivity of rice starch-based SPE was found in the addition of 45% of sodium iodide (NaI) salts with an ionic conductivity of 4.79×10^{-4} S/cm. In this study, further research will be studied regarding the ionic conductivity of the addition of other sodium salts, namely sodium acetate salt (CH_3COONa) which is more environmentally friendly, harmless, and abundant in nature. The effect of adding sodium acetate salts will be further analyzed through XRD, FTIR, TGA, Soil Burial Test, EIS, and CV.

Experiments

The solution casting technique was used to prepare SPE using 2 grams rice starch as host polymer, 20 ml distilled water with 99% purity as solvent, 1.36 ml glycerol 85% purity Merck CAS no 56-81-5 as plasticizer, and various concentration of anhydrous sodium acetate salt (CH_3COONa) 99% purity Merck CAS no 127-09-3 as ionic dopant. The salt variation used in this study were 0%, 15%, 25%, 35%, and 45% by weight of sodium acetate salt to the weight of rice starch. Sample with no addition of salt (0%) will use as a control sample.

All samples were characterized by XRD Olympus BTX-534 to study the crystal structure, FTIR Thermo Scientific Nicolet IS5 with ATR Id7 to study the functional group, TA Instruments SDT 650 to study the temperature decomposition, Soil Burial Test to study the biodegradability, and AutoLab Electrochemical Impedance Spectroscopy (EIS) to study the resistance of SPE. EDLC performance analysis was performed by measuring specific capacitance through cyclic voltammetry using AutoLab instrument with 2 system electrodes. The EDLC was fabricate using symmetric EDLC with 2 graphite electrodes separated by the SPE.

Result and Discussion

X-Ray Diffraction (XRD). Based on the result of XRD in Figure 1, there are sharp and non-widening diffraction peaks were found at angles of 2θ = 11.5°, 11.7°, 19.8°, 22.6°, and 30° in diffractogram of CH_3COONa salt. In rice starch can be found diffraction peaks at angles of 2θ = 15°, 17.2°, 18°, and 22.9° that categorized as type A crystalline and diffraction peak at angles of 2θ = 5.5°, 20°, and 26.6° categorized as type B crystalline. Thus, the crystal structure of starch can be categorized as type C which consist of type A and type B. In crystalline type C, the XRD pattern can contain various superpositions of diffraction peaks that depend on the ratio of composition between polymorphs [9]. According to Yang et al. [10], the peak of 2θ -angle diffraction located at 17° is identified as amylose and at 20° as amylopectin. During the gelatinization process, the amylose chain is released, the viscosity increases, and the amorphous structure increases [11]. The difference in diffraction peaks between rice starch and pure SPE (sample 0%) is found in the presence of diffraction peaks at an angle of 2θ = 15° in rice starch, while in pure SPE sample there is no peaks at that angle of 2θ. The difference is also clearly visible at angles of 2θ = 17.2°, 18°, and 22.9° in rice starch whose peaks widen at a sample of 0% indicated at angles of 2θ = 17.3° and 21.9°.

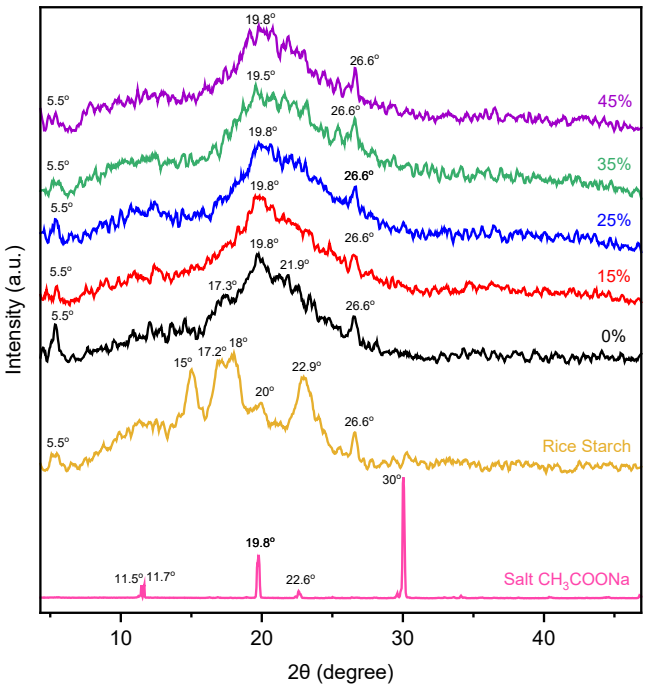

Fig. 1. X-Ray diffraction patterns of CH_3COONa, rice salt, and SPE with variation of the salt concentration

The addition of CH_3COONa salt to a pure SPE sample based on Figure 1 influences the crystal structure of the sample. Changes in the crystal structure are located at angles of 2θ = 17.3° and 21.9° which indicates the presence of diffraction peaks in pure SPE samples (0%), but these peaks are not present in SPE samples with the addition of salts. The change indicates that the addition of salt makes the crystal structure of SPE more amorphous [12]. When the amount of salt added is continuously increased, XRD diffraction does not show significant changes. To find out the most amorphous crystal structure, it is necessary to calculate the crystal size using the Debye-Scherrer equation expressed by Eq. (1).

$$D = \frac{0.9\,\lambda}{\beta\,cos\theta} \tag{1}$$

where D is the estimated crystal size (nm), λ is the wavelength of X-rays (nm), β is full width half-maximum (FWHM) (°), and θ is the peak angle of diffraction (°) [13]. The FWHM value of the sample increased along with the increase in the concentration of sodium acetate salt.

Table 1. Crystal size calculation

Sample	2θ (°)	θ (°)	FWHM (°)
0% Salt	19.786	9.893	8.562
15% Salt	19.829	9.914	8.729
25% Salt	19.786	9.893	8.874
35% Salt	19.572	9.786	10.358
45% Salt	19.786	9.893	9.162

Based on Table 1, the highest value of FWHM is reached by the sample SPE with the addition 35% salt. The greater the FWHM value means that the increment of the amorphous phase on the sample is due to the addition of plasticizer and salt. However, SPE samples with 45% salt experienced a decrease in FWHM values due to crystallization. It is because the host polymer could not accommodate an excess amount of salt [14].

Fourier Transform Infrared (FTIR). Based on Fig. 2, the pure SPE spectrum, represent by a black line color, has a wide absorption band in single bond region at 3274 cm^{-1}. The region around 3274 cm^{-1} indicates the presence of a hydroxyl group O-H stretching. At wavenumber of 2929 and 2887 cm^{-1} there are also peak for C-H stretching. Meanwhile, in triple and double bond region, there is no absorption band. This suggests that the SPE do not have a functional group with a triple bond nor double bond. In addition, the peak at 1648 cm^{-1} is associated with water function group, O-H bending.

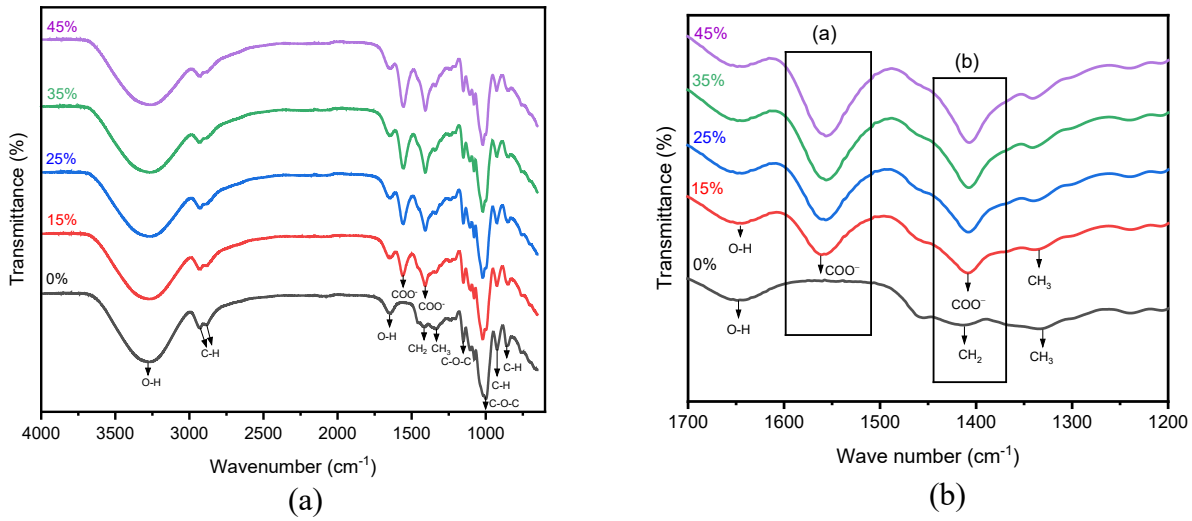

Fig. 2. FTIR spectrum of (a) SPE with variation of sodium salt concentration and (b) enlargement wavenumber 1200 – 1700 cm^{-1}

In the fingerprint region there are many functional groups such as CH_2 bending at 1414 cm^{-1}, CH_3 bending at 1335 cm^{-1}, and several typical starch functional groups at range 1300-1000 cm^{-1}. That typical starch functional groups are C–O-H, C–O–C by glycosidic bonds, C–O, and C–C [15]. It is specified as C-O-C stretching at 1151 cm^{-1}, secondary alcohol (C-O-H) stretching at 1105 cm^{-1}, primary alcohol (C-O-H) stretching at 1077 cm^{-1}, and glycosidic bond (C–O–C) stretching with high intensity at 1001 cm^{-1}. In addition, there are also peak of C-H bending groups at 924, 860, and 760 cm^{-1}. Figure 2 (b) shows the enlargement area of FTIR spectrum. In sections (a) at wavenumber 1560 cm^{-1} and (b) at 1408 cm^{-1} there are new absorption bands and the peak increase along with the addition of CH_3COONa salt concentrations. It can be attributed to carbonyl bonds, with two peaks detected due to the presence of two resonant structures [16]. The vibration of the carbonyl group was declared by Habka et al. [17] to be an antisymmetric stretching carboxylate (COO–) group at 1560 cm^{-1} and a carboxylate group (COO–) symmetric stretching at 1408 cm^{-1}. The presence of the COO function groups indicates the occurrence of acetyl group substitution due to starch acetylation. The substitution of acetyl groups in starch increases the resistance to retrogradation [18]. Thus, it makes the amorphous structure more stable.

Thermogravimetric Analysis (TGA). Figure 3 shows that all samples have single-step decomposition. In sample 0% salt, the weight of the sample experienced a drastic decrease at 283.16 °C and it is referred as the decomposition temperature.

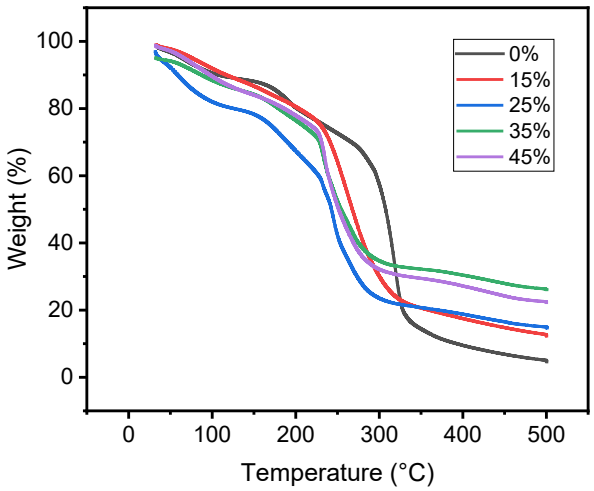

Fig. 3. TGA Thermogram of SPE

When the sample was added with salt, the decomposition temperature shifted to a lower temperature. It occurs due to the complexity between polymers and salts which increases segmental flexibility in the polymer matrix [6]. In other words, the addition of CH_3COONa causes a weak bond between Na^+ ions and hydroxyl groups in starch polymers. Along with the increasing concentration of salt, there is no significant change in the decomposition temperature. The difference can be seen in the sample of 25% of salts that slightly experienced weight loss at 158.86 °C. Since the weight loss is quite drastic at 228.10 °C, it is set to be the decomposition temperature of the sample.

Soil Burial Test. This biodegradability test focuses on analyzing the effect of salt addition on the degree of degradability of the film. The selection of the test time is determined based on the minimum time that one of the samples can be perfectly degraded. The results of the biodegradability test showed that within 28 hours the sample 45% salt had been fully degraded while the sample of 0% salt was still not degraded. If the testing time is extended, the sample will degrade perfectly because rice starch is an organic compound. This is because microorganisms in the soil use organic compounds as a source of nutrients for their metabolism [19].

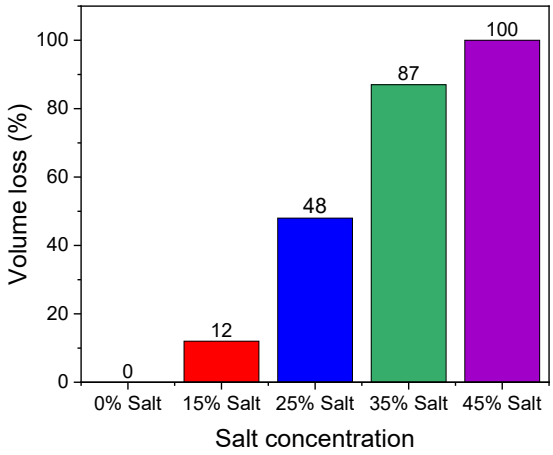

Fig. 4. Volume loss of SPE samples within 28 hours

The calculation of volume loss was chosen compared to weight loss because the samples that have been planted in the soil are difficult to clean. Therefore, an approach is made to the remaining area of the area and multiplied by the thickness of the sample. Based on Figure 4, it is known that the higher the salt concentration, the greater the volume lost from SPE due to biodegradation. So that the maximum biodegradability occurs at the highest salt concentration [20]. The increase in biodegradability is due to the interaction of sodium salts to the starch hydroxyl group. In addition, the reaction of acetylation also affects the biodegradability of starch. The large biodegradability of the

film results from the insertion of acetyl groups that can reduce the inter- and intramolecular interactions promoted by hydrogen bonds [21].

Electrochemical Impedance Spectroscopy (EIS). This impedance study focused on calculating the value of bulk resistance obtained through the Nyquist Plot which is a graph that presents impedance value data (Z) consisting of a real impedance (Z') and an imaginer impedance (Z"). On the Nyquist plot, there is a semicircle curve at high frequency describing the process of ion transfer on SPE and a linear curve at low frequency describing the diffusion process.

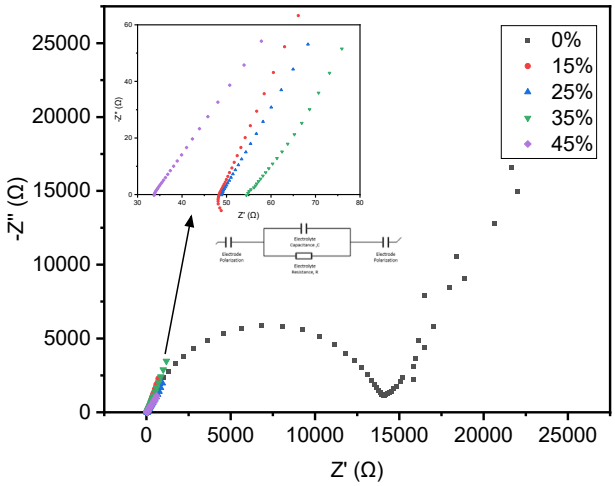

Fig. 5. Nyquist plot at SPE at room temperature

Based on the Fig. 5, the semicircle obtained by the SPE sample of 0% salt has a much larger shape than the SPE sample with the addition of salt. The larger the semicircle indicates that the process of ion diffusion is proceeding slowly due to the large resistance. In the salt addition sample, the semicircle looks very small indicating that the resistance is significantly decreased. The difference between the semicircle's initial and final intersections at the real impedance axis (Z') is expressed as bulk resistance (Rb). The ionic conductivity is calculated using Eq. (2).

$$\sigma = \frac{t}{A \times R_b} \tag{2}$$

where t is the thickness of the sample (cm), A is the surface area of the sample (cm^2), R_b is the bulk resistance (Ω), and σ is the ionic conductivity (S/cm).

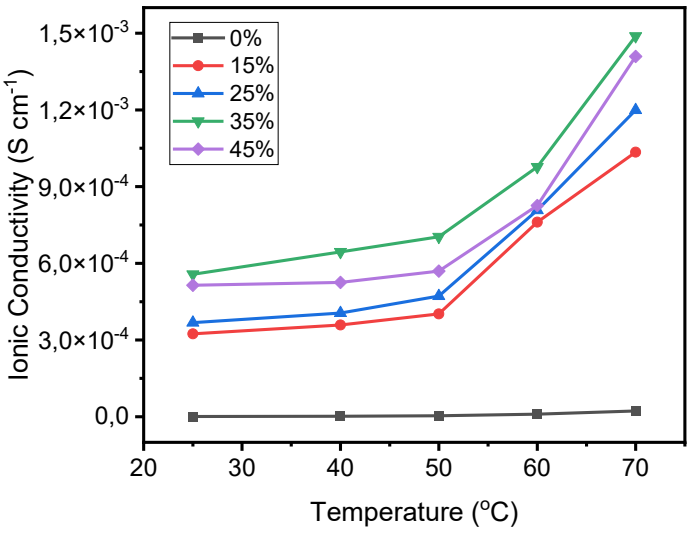

Fig. 6. Temperature-dependent of Ionic Conductivity

Based on the Fig. 6, the resistance of the sample begins to decrease when a pure SPE sample is added with CH_3COONa salt. The decrease in resistance is due to the presence of Na^+ in the polymer which can increase the ionic conductivity. Na^+ cations have a weak bond with O^- in polymers, making Na^+ will easily jump to other vacant sites to produce an ionic conduction mechanism [22]. An increase in salt concentration will make an increase in the concentration of ions in the polymer matrix so that the ionic conductivity will be increased [7]. Based on the tests that have been carried out, SPE samples with a concentration of 35% salt have the smallest R_b with a value of 23.63 Ω and the largest ionic conductivity with a value of 5.57×10^{-4} S cm^{-1}. The continuous increase in salt concentration does not necessarily increase ionic conductivity as it happens in the sample of adding 45% salt. In samples 45% of salts the ionic conductivity drops after reaching the highest value in the sample of 35% salt. The decrease in ionic conductivity at high salt concentrations is caused by ion aggregation which causes overcrowded ions in the polymer matrix so that ion mobility decreases [23].The impedance study was also carried out at elevated temperatures to study the temperature-dependent of ionic conductivity. In Fig. 6, it can be known that an increase in temperature can increase ionic conductivity. The higher the temperature, the lower the resistance of the SPE. It is because bonds of O and Na will be more easily released at higher temperatures so that the ion movement will increase. In addition, the expansion of the film volume due to the increase in temperature makes more space for the ion to mobile so that the ionic conductivity increases [24]. The temperature-dependent of ionic conductivity was further studied using Arrhenius modeling.

$$\ln \sigma = \frac{-Ea}{RT} + \ln A \tag{3}$$

From Eq. (3) can be known the relationship between activation energy to ionic conductivity. The value of the activation energy (*Ea*) is calculated based on the linearization of the Arrhenius equation. The value of the activation energy can be obtained from the slope (gradient) of the plot ln ionic conductivity vs 1000/T.

Table 4. Activation energy of SPE

Sample	Slope	Ea (J/mol)
0% Salt	-7.621	63.357
15% Salt	-2.724	22.649
25% Salt	-2.703	22.476
35% Salt	-2.121	17.636
45% Salt	-2.148	17.861

The activation energy value indicates the quantity of energy required by the ion to be able to move on the polymer matrix. The decrease in activation energy shows that ion movement goes easier and faster. Based on Table 4, an increase in the concentration of CH_3COONa salts plays a role in lowering activation energy.

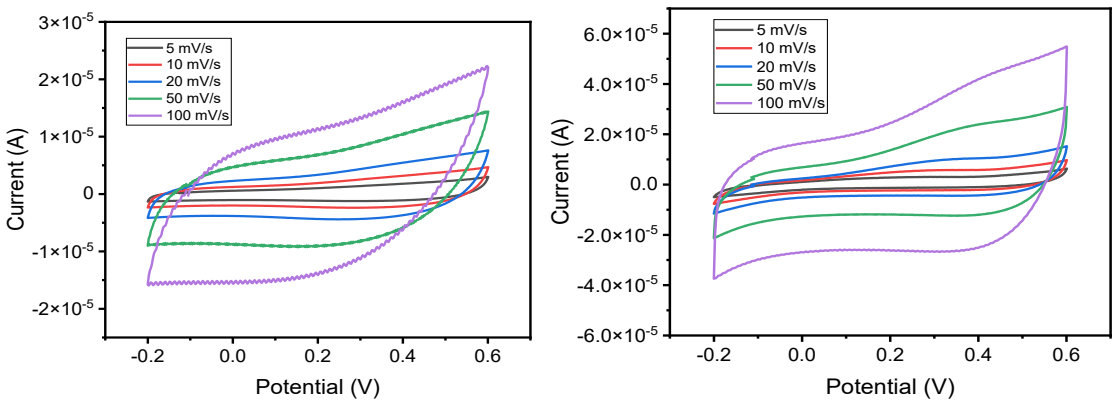

Fig. 8. Scan Rate Test Sample (a) 0% Salt, (b) 35% Salt

Cyclic Voltammetry (CV). EDLC performance tests were performed with Cyclic Voltammetry (CV) to calculate specific capacitance. The shape of the curve due to the change in scan rate did not undergo significant changes with no redox reaction peak found as shown in Figure 8. It shows that the SPE with a graphite electrode can run at low or high scan rates from the range of 5 mV/s to 100 mV/s. In this study, a scan rate of 10 mV/s was used to determine the changes occurred when the EDLC running with 50 cycles.

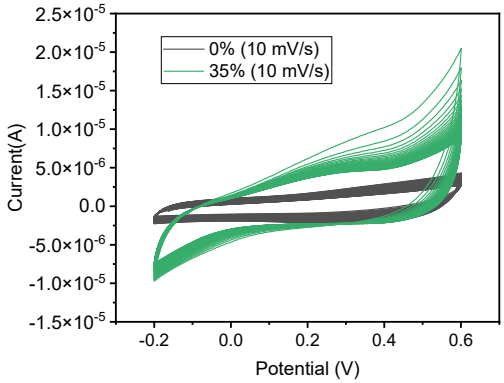

Fig. 9. CV with 50 Cycles at 10 mV/s of the SPE sample with 0% and 35% salt concentration

In the Fig. 9, a curve with a green line represents the behavior of a sample of 35% salt in 50 cycles whose area decreases slightly in the initial cycle. However, after cycle 10 the area is more stable. The decrease in the area that occurs may be caused by ion aggregation during the charge-discharge process [26]. In the initial cycle, the ions from sodium have very high mobility in the polymer matrix and after 10 cycles, ion aggregation tend to decrease thus their mobility is more stable. The calculation of the capacitance value is carried out using Eq. (4).

$$C_p = \frac{\int I\, dV}{2mv(V_2 - V_1)} \tag{4}$$

where C_p is the specific capacitance (F/g), m is the electrode mass (gram), v is the scan rate (mV/s), V_1 and V_2 are the initial and final potentials and $\int I\, dV$ is the CV area.

Table 5. Specific Capacitance of EDLC Using SPE

Sample	Area (A.V)	Scan rate (mV/s)	Specific Capacitance (F/g)
0% Salt	1.22×10^{-6}	10	0.0047
35% Salt	6.73×10^{-6}	10	0.0240

Based on the Table 5, the area of the sample is 35% salt bigger than the sample 0% salt. The specific capacitance is directly proportional to the area, making the specific capacitance of 35% salt reach 0.0240 F/g. In this study, the addition of CH_3COONa salt was able to increase the specific capacitance up to 5 times. Na^+ dispersed in the matrix polymer can improve the adsorption and desorption processes in the electrolyte-electrode interface during the charging and discharging process.

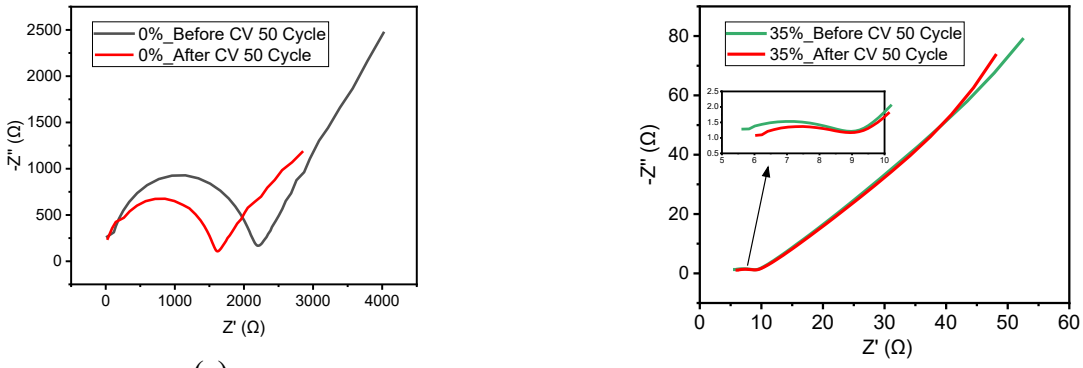

(a) (b)

Fig. 11. EIS Before and After 50 Cycles Sample (a) 0% Salt, (b) 35% Salt

In the picture above, there is a Nyquist plot that shows the difference in the size of the semicircle. In the 0% salt sample there was a significant decrease in semicircle size from 2199.6 Ω to 1798.5 Ω after 50 cycles. The decrease in resistance is indicated due to the influence of the ion adsorption and desorption process during charge-discharge which makes the SPE surface more conductive. Whereas in a sample of 35% salt, the change in resistance tended to be small from 7.199 Ω to 6.267 Ω which showed that the 50 cycles did not significantly affect the mobility of ions in the polymer matrix.

Summary

Synthesis SPE from rice starch makes the crystal structure of the starch turn amorphous through a gelatinization process. The addition of sodium acetate salt (CH_3COONa) plays a role in improving the amorphous structure of SPE. The SPE sample with 35% salt has the most amorphous structure. The addition of salts to the sample was evidenced by the presence of new functional groups at wavenumbers 1560 cm^{-1} and 1408 cm^{-1} which were identified as carboxylate functional groups (COO^-) antisymmetric stretching and carboxylate groups (COO^-) symmetric stretching. The influence of salt addition also affects decreasing the decomposition temperature and increasing the biodegradability of the sample. The effect of salt addition was seen in a significant decrease in bulk resistance of SPE samples from 14112 Ω at 0% salt to 35.41 Ω at 15% salt. An increase in salt concentration indicates a decrease in resistance thus ionic conductivity becomes increased. The highest ionic conductivity is achieved by a sample of 35% of salts with a value of 5.57×10^{-4} S cm^{-1}. The fabrication of the EDLC is carried out with 2 graphite electrodes separated by SPE 35% salt as a solid electrolyte. CV test results showed 5 times increase in capacitance when using SPE 35% salt compared to SPE 0% salt.

Acknowledgment

The author would like to thank the Mechanical Engineering Department and Chemical Engineering Department, Faculty of Industrial Technology, Universitas Pertamina for technical and financial support for this research.

References

[1] B. K. Roy, I. Tahmid, T. U. Rashid, Chitosan-based materials for supercapacitor applications: a review, J. Mater. Chem. A. 9 (2021) 17592–17642.

[2] M. Rayung,M. M. Aung, S. C. Azhar, L. C. Abdullah, M. S. Su'ait, A. Ahmad, S. N. A. M. Jamil, Bio-Based Polymer Electrolytes for Electrochemical Devices: Insight into the Ionic Conductivity Performance, Materials. 13 (2020) 838.

[3] L. P. Teo, M. H. Buraidah, A. K. Arof, Development on Solid Polymer Electrolytes for Electrochemical Devices, Molecules. 26 (2021) 21.

[4] M.K. Marichelvam, M. Jawaid, M. Asim, Corn and Rice Starch-Based Bio-Plastics as Alternative Packaging Materials, Fibers. 7 (2019) 4.

[5] N. Singh, J. Singh, L. Kaur, N. Singh Sodhi, B. Singh Gill, Morphological, thermal and rheological properties of starches from different botanical sources, Food Chem. 81 (2003)219-231.

[6] M. H. Khanmirzaei, S. Ramesh, K. Ramesh, Effect of different iodide salts on ionic conductivity and structural and thermal behavior of rice-starch-based polymer electrolytes for dye-sensitized solar cell application, Ionics (Kiel). 21 (2015) 2383–2391.

[7] F. F. Awang, M. F. Hassan, K. H. Kamarudin, Corn starch doped with sodium iodate as solid polymer electrolytes for energy storage applications, Acta Polytech. 61 (2021) 497–503.

[8] Z. Osman, K. B. Md Isa, A. Ahmad, L. Othman, A comparative study of lithium and sodium salts in PAN-based ion conducting polymer electrolytes, Ionics (Kiel). 16 (2010) pp. 431–435.

[9] K. Dome, E. Podgorbunskikh, A. Bychkov, and Lomovsky, Changes in the Crystallinity Degree of Starch Having Different Types of Crystal Structure after Mechanical Pretreatment, Polymers. 12 (2020) 3.

[10] K. Yang, X. Luo, Y. Zhai, J. L., K. C., X. S., X. Wu, Y. Li, Z. Chen, Influence of sodium alginate on the gelatinization, rheological, and retrogradation properties of rice starch, Int. J. Biol. Macromol. 185 (2021) 708–715.

[11] E. J. Vernon-Carter, J. Alvarez-Ramirez, L. A. Bello-Perez, C. Roldan-Cruz, A. Garcia-Hernandez, and L. Huerta, The order of addition of corn starch/lithium perchlorate/glycerol affects the optical, mechanical, and electrical properties of a solid polymer electrolyte," Ionics (Kiel). 23 (2017) 3111–3123.

[12] A. C. W. Ong, N. A. Shamsuri, S. N. A. Zaine, D. Panuh, M. F. Shukur, Nanocomposite polymer electrolytes comprising starch-lithium acetate and titania for all-solid-state supercapacitor, Ionics (Kiel). 27 (2021) 853–865.

[13] Y. L. Yap, A. H. You, L. L. Teo, Preparation and characterization studies of PMMA–PEO-blend solid polymer electrolytes with SiO_2 filler and plasticizer for lithium ion battery, Ionics (Kiel). 25 (2019) 3087–3098.

[14] S. S. Priya, M. Karthika, S. Selvasekarapandian, R. Manjuladevi, Preparation and characterization of polymer electrolyte based on biopolymer I-Carrageenan with magnesium nitrate, Solid State Ionics. 327 (2018) 136–149.

[15] I. Govindaraju, G. Y. Zhuo, I. Chakraborty, S. K. Melanthota, S. S. Mal, B. S., V. J. Baruah, K. K. Mahato, N. Mazumder, Investigation of structural and physico-chemical properties of rice starch with varied amylose content: A combined microscopy, spectroscopy, and thermal study, Food Hydrocoll. 22 (2022) 107093.

[16] B. B. Cazula, E. C. Meurer, A. M. Fortes, A. P. Tonin, L. J. Gasparrini, C. I. Yamamoto, H. J. Alves, Concomitant Production of Hydrogen, Sodium Acetate, and Polymerized Species from Non-Catalytic Ethanol Dehydrogenation," J. Braz. Chem. Soc. 31 (2019) 126-134.

[17] S. Habka, T. Very, J. Donon, V. Vaquero-Vara, B. Tardivel, F. Charnay-Pouget, M. Mons, D. J. Aitken, V. Brenner, E. Gloaguen, Identification of ion pairs in solution by IR spectroscopy: crucial contributions of gas phase data and simulations, Phys. Chem. Chem. Phys. 21 (2019) 12798–12805.

[18] J. I. Morán, V. P. Cyras, S. L. Giudicessi, R. Erra-Balsells, A. Vázquez, Influence of the glycerol content and temperature on the rheology of native and acetylated starches during and after gelatinization, J. Appl. Polym. Sci., 120 (2011) 3410–3420.

[19] M. M. Abe, M. C. Branciforti, M. Brienzo, Biodegradation of Hemicellulose-Cellulose-Starch-Based Bioplastics and Microbial Polyesters, Recycling , 6 (2021) 22.

[20] M. Selvakumar, D. K. Bhat, LiClO4 doped cellulose acetate as biodegradable polymer electrolyte for supercapacitors, J. Appl. Polym. Sci. 110 (2008) 594–602.

[21] R. Colussi, V. Z. Pinto, S. L. M. E. Halal, B. Biduski, L. Prietto, D. D. Castilhos, E. D. R. Zavareze, A. R. G. Dias, Acetylated rice starches films with different levels of amylose: Mechanical, water vapor barrier, thermal, and biodegradability properties, Food Chem. 221 (2017) 1614–1620.

[22] J. I. C. Wong, S. Ramesh, H. K. Jun, C. Liew, Development of poly(vinyl alcohol) (PVA)-based sodium ion conductors for electric double-layer capacitors application, Mater. Sci. Eng. B. 263 (2021) 114804.

[23] M. N. Hafiza, M. I. N. Isa, Solid polymer electrolyte production from 2-hydroxyethyl cellulose: Effect of ammonium nitrate composition on its structural properties, Carbohydr. Polym. 165 (2017) 123–131.

[24] V. S. Kumaran, H. M. Ng, S. Ramesh, K. Ramesh, B. Vengadaesvaran, A. Numan, The conductivity and dielectric studies of solid polymer electrolytes based on poly (acrylamide-co-acrylic acid) doped with sodium iodide, Ionics (Kiel). 24 (2018) 1947–1953.

[25] S. B. Aziz, E. M. A. Dannoun, A. R. Murad, K. H. Mahmoud, M. A. Brza, M. M. Nofal, K. A. Elsayed, S. N. Abdullah, J. M. Hadi, M. F. Z. Kadir, Influence of scan rate on CV Pattern: Electrical and electrochemical properties of plasticized Methylcellulose: Dextran (MC:Dex) proton conducting polymer electrolytes, Alexandria Eng. J. 61 (2022) 5919–5937.

[26] E. M. A. Dannoun, S. B. Aziz, S. N. Abdullah, M. M. Nofal, K. H. Mahmoud, A. R. Murad, R. M. Abdullah, M. F. Z. Kadir, Characteristics of Plasticized Lithium Ion Conducting Green Polymer Blend Electrolytes Based on CS: Dextran with High Energy Density and Specific Capacitance, Polymers. 13 (2021) 13.